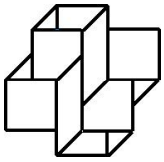

Laboratório Nacional de Computação Científica

Programa de Pós-Graduação em Modelagem Computacional

Standard deviation of a staggered quantum walk on a line of diamonds

Cauê Francisco Teixeira da Silva

Petrópolis, RJ - Brasil

Maio de 2018

Cauê Francisco Teixeira da Silva

Standard deviation of a staggered quantum walk on a line of diamonds

Dissertation submitted to the examining committee in partial fulfillment of the requirements for the degree of Master of Sciences in Computational Modeling.

Laboratório Nacional de Computação Científica

Programa de Pós-Graduação em Modelagem Computacional

Supervisor: Renato Portugal

Petrópolis, RJ - Brasil

Maio de 2018

Silva, Cauê Francisco Teixeira da
S586s Standard deviation of a staggered quantum walk on a line of diamonds / Cauê Francisco Teixeira da Silva -- Petrópolis, RJ. : Laboratório Nacional de Computação Científica, 2018.
48 p. : il. ; 29 cm.

Orientador: Renato Portugal.

Dissertação (Mestrado) – Laboratório Nacional de Computação Científica, 2018.

1.Computadores quânticos 2. Tesselação de gráficos 3. Caminhada quântica escalonada 4. Desvio padrão I. Renato Portugal II. MCTIC/LNCC; III.Título

CDD – 004.1

Cauê Francisco Teixeira da Silva

Standard deviation of a staggered quantum walk on a line of diamonds

Dissertation submitted to the examining committee in partial fulfillment of the requirements for the degree of Master of Sciences in Computational Modeling.

Approved by:

Prof. Renato Portugal, D. Sc.
(Presidente)

Prof. Gilson Antônio Giraldi, D. Sc.

Prof. Severino Collier Coutinho, Ph. D.

Petrópolis, RJ - Brasil
Maio de 2018

Dedication

Para minha mãe

Acknowledgements

À minha mãe por toda dedicação, amor e carinho. Mas principalmente por saber que "quem ama educa", sou muito priveligiado por ter crescido com uma educação num sentido tão amplo.

À minha família por todo o apoio. Ter vocês ao meu lado é maravilhoso. Cada um de vocês é fundamental na minha vida, mas não posso deixar de citar meu pai, Raphael, tio Totõe e as tias Angela, Dindinha, do Carmo e Odete.

Ao meu orientador Renato Portugal pela ótima orientação, paciência e todo apoio. Serei para sempre grato por todo apoio que você me deu neste período.

Aos amigos Arthur, Diogo e Luiz por todas conversas nesses dois últimos anos que me fizeram crescer tanto como pessoa.

Aos amigos do LNCC Aaron, Felipe, Leandro, Lucas, Luiza e Nicolau por toda força, todo companheirismo e toda camaradagem.

Aos colegas do grupo de quântica Bruno, Pedro e Tharso, por toda ajuda.

Ao CNPq, pelo apoio financeiro. Agradeço também ao LNCC e seus pesquisadores e funcionários.

"Caminhante não há caminho,
se faz caminho ao andar."
(Antonio Machado)

Abstract

The discovery of the quantum mechanics changed the physics world. Newton's laws of motion cannot be applied to very small physical systems. The quantum mechanics has many applications, one of them is the quantum computation, which was discovered in the 80's and has steadily grown from that time to nowadays. One powerful tool of quantum computation is the quantum walk, which is the quantum version of random walk. In this work, we study some quantum walk models. The coined model was the first one to be proposed, this model has a quadratic larger position standard deviation compared to the one of the random walk. The second model is the staggered quantum walk, which was proposed recently. This model makes a partition of the vertices of the graph into cliques, and a partition is called tessellation, establishing a new problem of graph theory, related to the problem of graph coloring. We study 2-tessellable graphs and prove a new theorem in graph theory. An expression of the standard deviation of a staggered quantum walk on the line-of-diamond graph is obtained using a special basis, which is derived from the staggered Fourier transform.

Keywords: staggered quantum walk. graph tessellation. standard deviation.

Resumo

A descoberta da mecânica quântica mudou o mundo da física. As leis de Newton do movimento não podem ser utilizadas para sistemas físicos muito pequenos. A mecânica quântica tem muitas aplicações, uma delas é a computação quântica, que foi descoberta na decada de 80 e tem crescido constantemente desde aquela época até hoje em dia. Uma forte ferramenta da computação quântica é a caminhada quântica, que é a versão quântica da caminhada aleatória. Neste trabalho, estudamos alguns modelos de caminhadas quânticas. O modelo com moeda foi o primeiro modelo proposto, este modelo possui um desvio padrão da posição quadraticamente maior em relação ao da caminhada aleatória. O segundo modelo é a caminhada quântica escalonada, proposto recentemente. Este modelo particiona os vértices do grafo em cliques, tal partição é chamada de tesselação, estabelecendo um novo problema em teoria dos grafos, relacionado ao problema de coloração de grafos. Estudamos grafos 2-tesseláveis e provamos um novo teorema em teoria dos grafos. Uma expressão do desvio padrão de uma caminhada quântica escalonada no grafo linha-de-diamantes é obtida usando uma base especial, que deriva da transformada de Fourier escalonada.

Palavras-chave: caminhada quântica escalonada. tesselação de grafos. desvio padrão.

List of Figures

List of Tables

Contents

1 Introduction

Suppose that a particle in a flat smooth surface is pushed by a force with random magnitude and direction at every second. The Brownian motion can be described by random forces and was discovered by Robert Brown in 1827. He noted that the movement of a pollen in a water surface can be described by random forces pushing the pollen. Brown observed that inorganic particles exhibited this same behavior. With a microscope, he observed that the particle receives collisions with smaller particles of the fluid generating the Brownian movement.

The Brownian movement can be mathematical modeled by random walks, which was formulated for the first time by Pearson in 1905. We can imagine a particle walking randomly on a line, in each step it has a probability to go rightward or leftward. The description of the walk of the particle cannot be done in a deterministic way, only in a probabilistic way. Random walks can be applied in physics, psychology, economy and computer science

One way of simulating a random walk on a line is similar to the Mach-Zehnder modulator experiment (VIEIRA, 2014). We position 6 beam splitters[1] and 4 photometers[2] as Figure 1 shows. A light beam is launched in the first beam splitter such that the light passes through all beam splitters and is measured at the end by the photometers. From top to bottom we have that the intensity of light is divided with 1/8, 3/8, 3/8 and 1/8. Changing this experiment to quantum conditions (photon emissions), it arises a difference on the measurements of the photometers. It can be verified experimentally that the probability of the photon be detected in the photometers, from top to bottom, is 1/8, 1/8, 5/8 and 1/8. This difference between the classical and quantum world is generated by the quantum interference.

The evolution of computers makes use of smaller and smaller circuits as time passes. In the early 80's, some researchers asked themselves what would happen when the circuits became so small that the physics involved in the computer circuits would pass from classical mechanics to quantum mechanics. This research resulted in the development of the quantum computation, which possesses as its starting point the article of Deutsch (DEUTSCH, 1985). From 1985 to today the interest in quantum computation increased significantly. Two papers collaborated enormously for this interest. First, Shor (SHOR, 1994) presented a quantum algorithm for integer factorization, which is exponentially faster than the known classical algorithms. Second, Grover (GROVER, 1996) presented a search algorithm with quadratic gain. These two works are important because they used,

[1] Half the light goes straight through and half is mirrored.
[2] Photometer is an instrument that measures light intensity.

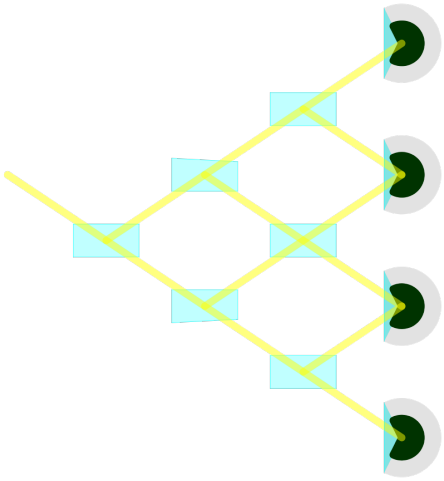

Figure 1 – An experiment that simulate the random walk on a line. The yellow lines represent a light beam, the blue rectangles represent beam splitters and the pieces of circle represent the photometers.

for the first time, two techniques very important in quantum computation, the quantum Fourier transform and amplitude amplification, respectively.

Quantum walks is a third important technique in quantum algorithms. Quantum walks, as defined for the first time by Aharanov et al. (AHARONOV; DAVIDOVICH; ZAGURY, 1993), which use an additional coin space and discrete time. A continuous time version was introduced by Farhi et al. (FARHI; GUTMANN, 1997). Quantum walks gained importance due to many works. One is the work of Childs et al. (CHILDS et al., 2003). He used quantum walks on the graph that is composed of two trees with height n connecting their leafs randomly. He showed that the quantum walk goes from a root to the other with an exponential speedup compared to the classical random walk. Childs also proved (CHILDS, 2009) that quantum walks are universal for quantum computation, that is, any quantum algorithm can be described as a random walk on a graph.

Despite the success of the coined quantum walks, other models without the use of a coin were proposed. Szegedy (SZEGEDY, 2004) proposed a model of quantum walk on a bipartite graph that is generated by a given graph. More recently Portugal et al. (PORTUGAL et al., 2016) proposed another model that generalizes the Szegedy model, the staggered model. Such model received an extension (PORTUGAL; OLIVEIRA; MOQADAM, 2017), using Hamiltonians. The idea of the staggered model is to associate a set of cliques of the graph with an operator that preserves the structure of the graph. From this model arises a new problem in graph theory, the graph tessellation (ABREU et al., 2017).

1.1 Contributions and organization

In chapter 2 we start with an introductory review of graph theory. After that, we study the graph tessellation and characterize the 2-tessellable graphs. In this chapter, we obtain a new theorem 2.2.5, which describes an algorithm new in the literature, as far as we know. In chapter 3 we introduce the coined walks (classical and quantum) and we compare their standard deviation, which is important because it is equal to the expected distance of the walker to its initial position. In chapter 4 we introduce the staggered quantum walk and study it on a line of diamonds. Moreover, we obtain the standard deviation for different Hamiltonians and use it to determine the Hamiltonian that gives to us the largest standard deviation. We confirm our analytical results with numerical simulations. We have submited two complete works to CNMAC 2018. One where we present the standard deviation of the staggered quantum walk on a line of diamonds, and the other where we characterize the triangle-free graphs that are 3-tessellable.

2 Graphs

In this chapter, we introduce some concepts important to us in graph theory. The first is the intersection graph, which is a graph generated from a family of sets. The second is the concept of tessellation. A tessellation of a graph is a partition of its vertices into cliques. A tessellation covers some edges of the graph, not necessarily all edges. In this case, we need more them one tessellation in order to define a tessellation cover. At the end of this chapter, we characterize the graphs for which 2 tessellations are enough to cover all edges. In the book (CHARTRAND, 1984) you can find more about graph theory.

2.1 Introduction to graphs

A *simple graph* (or *graph*) $G(V, E)$ is a nonempty set V of vertices and a set E of edges where each edge is a set of two vertices. We say that an edge *links* two vertices. We will denote the vertex set and edge set of a graph G by $V(G)$ and $E(G)$, respectively. We also denote the edge that links vertices u and v by uv. A first example of a graph is G, where $V(G) = \{v_1, v_2, v_3, v_4\}$ and $E(G) = \{v_1v_2, v_2v_3, v_2v_4, v_3v_4\}$. We can make a representation of a graph by a diagram (this representation is not unique). In Figure 2 a diagram representation of the graph G is shown, the horizontal edge links the vertices v_3 and v_4. In this manuscript we will refer the diagram representation simply as graph.

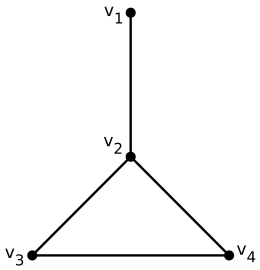

Figure 2 – Graph G.

If $uv \in E(G)$ then u and v are *adjacent* vertices. In this case, we say u is adjacent to v (or u is a neighbor of v). Note that u is adjacent to v if and only if v is adjacent to u. For example, in the graph G of Figure 2 the vertices v_1 and v_2 are adjacent. If $uv \notin E(G)$ then u and v are *nonadjacent* vertices. Two edges are adjacent if they share a common vertex. Again in G we have that v_2v_3 and v_2v_4 are adjacent.

Let G be a graph and $v \in V(G)$ be a vertex. The *degree* of vertex v is the number of edges in $E(G)$ that contains v. We denote the degree of a vertex v by $\deg_G(v)$. It is

equal the number of neighbors of v. A vertex of a graph is a *leaf* if its degree is 1. In Figure 2 we have $\deg_G(v_1) = 1$, $\deg_G(v_2) = 3$, $\deg_G(v_3) = 2$ and $\deg_G(v_4) = 2$.

Lemma 2.1.1 *Let G be a graph with $V(G) = \{v_1, ..., v_n\}$ and $|E(G)| = m$ edges. Then*

$$\sum_{i=1}^{n} \deg_G(v_i) = 2m.$$

Proof Each edge of the graph contributes twice to the sum, because each edge contains two vertices. □

If all vertices of a graph have the same degree r then the graph is *r-regular*. A graph is *complete* if every pair of vertices are adjacent, that is, it is $(n-1)$-regular, where n is the number of vertices. We denote the complete graph with n vertices by K_n. Figure 3 shows the complete graphs K_1, K_2, K_3 and K_4.

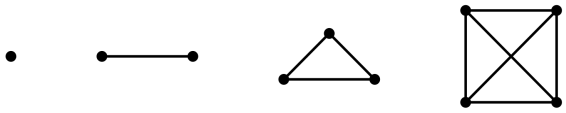

Figure 3 – Complete graphs K_1, K_2, K_3 and K_4.

A *subgraph* $G'(V', E')$ of a graph $G(V, E)$ is a graph such that $V' \subseteq V$ and $E' \subseteq E$. An *induced subgraph* is one that includes all the edges whose endpoints belong to the vertex subset. Comparing Figure 2 and Figure 4 we obtain that G' is a subgraph of G but it is not an induced subgraph, because the edge v_2v_3 should appear as in G''. A graph is *bipartite* if there is a partition of two sets of vertices such that it does not exist an edge linking vertices of the same partition, that is, the induced subgraphs of each set of the partition do not have any edge.

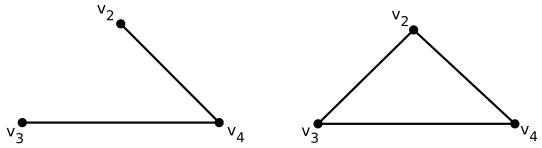

Figure 4 – Graph G' (left) and Graph G'' (right).

A *clique* is a set of vertices such that its induced subgraph is a complete graph. A *maximal clique* is a clique such that it is not possible to obtain a clique adding any other vertex. Note that each edge of a graph belongs to one maximal clique at least.

A *path* is a sequence of vertices such that two consecutive vertices always are linked by an edge. A graph is *connected* when there is a path between every pair of vertices, otherwise, it is called *disconnected*. A *cycle* is a path with three or more vertices such that the first and the last vertex are the same, without other repetition of vertices. The *n-cycle*

graph is a graph formed by a cycle with n vertices. The *n-wheel graph* is the graph formed by connecting a single vertex to all vertices of athe n-cycle.

An intersection graph is generated from a family of sets whose each set of this family is associated to a vertex, with an edge between two vertices when the corresponding sets have a nonempty intersection. Two important examples are the line graphs (intersection graph of the edges of a graph) and clique graphs (intersection graph of the maximal cliques of a graph). We denote by $L(G)$ and $K(G)$, respectively the line graph of G and the clique graph of G. There is a bijection between edges of G and vertices of $L(G)$.

A *multigraph* is an extension of the definition of graph that allows multiples edges between the same pair of vertices, that is, its edges is a multiset. Particularly, every graph is a multigraph. An n-multiedge is the induced subgraph by two vertices with n edges linking them.

A *adjacency matrix* A of a graph is a matrix such that the entries A_{ij} are the number of edges linking the vertices i and j.

The *n-wheel graph* is a graph formed by connecting a single vertex to all vertices of the n-cycle.

2.2 Characterization of the 2-tessellable graphs

A *tessellation* of a graph G is a partition of the vertex set $V(G)$ of the graph such that each element of the partition is a clique, not necessarily a maximal clique. Elements of the tessellation are called *polygons*. Since the tessellation is a partition, we have that the intersection of two polygons is empty and the union of all polygons is equal to $V(G)$. We say that the polygon P covers an edge of the graph if the endpoints of this edge belong to P. If a polygon of a tessellation $\mathcal{T}$ covers an edge e, we say that the tessellation $\mathcal{T}$ covers e. In Figure 5 we have in the left upper corner a graph with a red (continuous line) tessellation, in the right upper corner the same graph with a blue (dashed line) tessellation, and the lower part of the figure describes the same graph with these two tessellations. Note that the two tessellations together cover all edges of the graph.

A graph is n-tessellable if n tessellations are enough to cover all edges. A question that naturally arises from the study of the staggered quantum walk is which graphs are 2-tessellable. Portugal (PORTUGAL, 2016) has proved the following characterization.

Theorem 2.2.1 *(PORTUGAL, 2016) A connected graph is 2-tessellable if and only if its clique graph is 2-colorable.*

We know that a graph is bipartite if and only if it is 2-colorable. Then a graph is 2-tessellable if and only if its clique graph is bipartite. Let G be a graph and γ be a set of

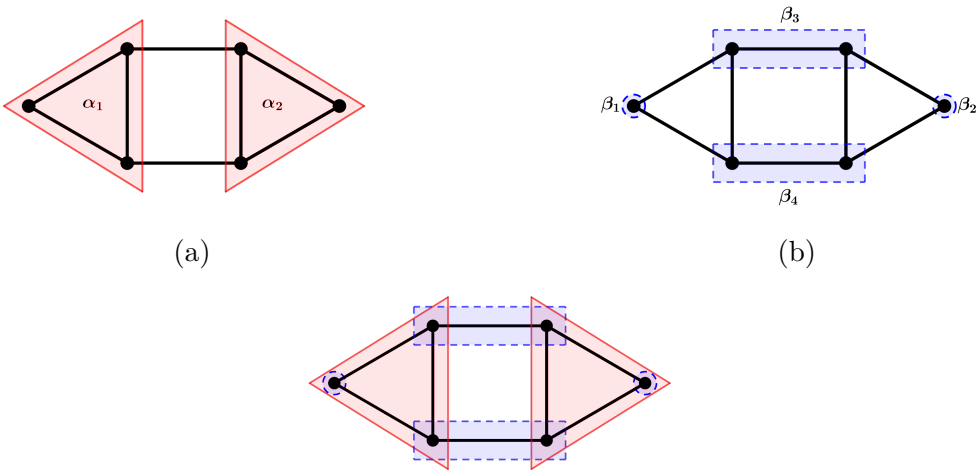

Figure 5 – Figure (a) show the red tessellation, figure (b) show the blue tessellation and figure (c) show that the graph is 2-tessellable

graphs, the graph G is γ-free if no induced subgraph of G is isomorphic to any graph of γ.

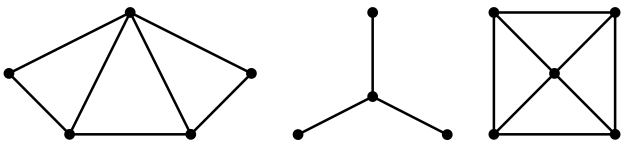

Figure 6 – 4-fan, claw, 4-wheel

Let β be the set of claw, 4-fan, 4-wheel (Figure 6), together with all n-cycles, where n is odd and greater than or equal to 5. Peterson (PETERSON, 2003) has proved the following theorem.

Theorem 2.2.2 *(PETERSON, 2003) $K(G)$ is bipartite if and only if G is β-free.*

From Proposition 2.1 and Theorem 2.2 we have a set of forbidden induced subgraphs. A graph G is 2-tessellable if and only if G is β-free.

If G is a multigraph, the underlying graph of G is a simple graph that is obtained from G by converting each multiple edge into a single edge.

Definition 2.2.3 *A **reduced subgraph** $R(G)$ of a multigraph G is a simple graph obtained from the underlying graph of G by deleting all its leafs.*

In Figure 7 we have an example of a multigraph G and it reduced subgraph $R(G)$. The vertices v_1 and v_3 were eliminated because they only have one neighbor v_2 and v_4,

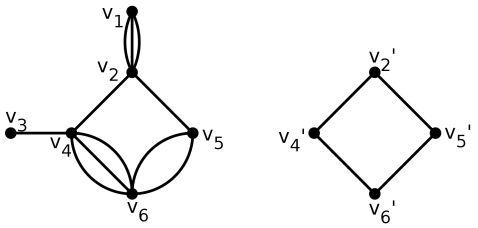

Figure 7 – A multigraph G (left) and its reduced subgraph $R(G)$ (right).

respectively . The remaining vertices are adjacent in $R(G)$ if they are in G. Moreover the multiple edges of G become single edges in $R(G)$.

Lemma 2.2.4 *Let H be a connected multigraph with at least three vertices. If H is triangle-free then $K(L(H))$ is the reduced subgraph of H.*

Proof Let H be a triangle-free multigraph. The incident edges to a vertex $v \in H$ form a clique C_v in $L(H)$. Now we show that C_v is maximal if and only if v has at least two neighbors. If v has only one neighbor v', C_v is not maximal because v' has another neighbor (H is connected with at least three vertices); it follows that C_v is a proper subclique of $C_{v'}$. If v has at least two neighbors, C_v is maximal because if by contradiction C_v is a proper subclique of a larger clique then there must exist an edge in H, that is not incident to v, sharing common vertices with all neighbors of v. Since this is not possible because H is triangle-free, we conclude that C_v is maximal.

Each vertex v of the reduced subgraph of H is associated with a maximal clique C_v in $L(H)$. Then, v is associated with a vertex $k_v \in K(L(H))$. Conversely, on the other hand, a vertex of $K(L(H))$ is associated with a maximal clique of $L(H)$, which is associated with a vertex of the reduced subgraph of H. Thus, we have established a bijection between the vertex set of $K(L(H))$ and the vertices of the reduced subgraph of H.

If v and v' are adjacent in the reduced subgraph of H then k_v and $k_{v'}$ are adjacent in $K(L(H))$ because there is an edge vv' in H whose corresponding vertex in $L(H)$ belongs to the intersection of C_v and $C_{v'}$. If k_w and $k_{w'}$ are adjacent in $K(L(H))$ then C_w and $C_{w'}$ have a nonempty intersection in $L(H)$, and w and w' are adjacent in the reduced subgraph of H. This shows that $K(L(H))$ and the reduced subgraph of H are isomorphic. □

Now we describe an algorithm that receives as input a graph G and its clique graph $K(G)$ which must be triangle-free, and returns as output a graph H such that H is a root graph of G, that is, $G = L(H)$.

Algorithm 1

Input: G and its triangle-free clique graph $K(G)$

Output: H

Step 1: : Initially H is a copy of $K(G)$ and for each vertex $v \in K(G)$ denote by r_v the corresponding vertex in H.

Step 2: Let r_v and r_w be two adjacent vertices of H. Let C_v and C_w be the respective maximal cliques of G. Let $m \geq 1$ be the number of vertices in the intersection of C_v and C_w. In H link vertices r_v and r_w with an m-multiedge. Repeat this step for all edges vw of $K(G)$.

Step 3: Let C_v be a maximal clique of G. Let n be the number of vertices of C_v which belongs only to C_v, that is, they do not belong to any other maximal clique. Link r_v with $r_{v_1}, ..., r_{v_n} \in H$ with 1-multiedge (edge). This step is repeated for all vertices $v \in K(G)$.

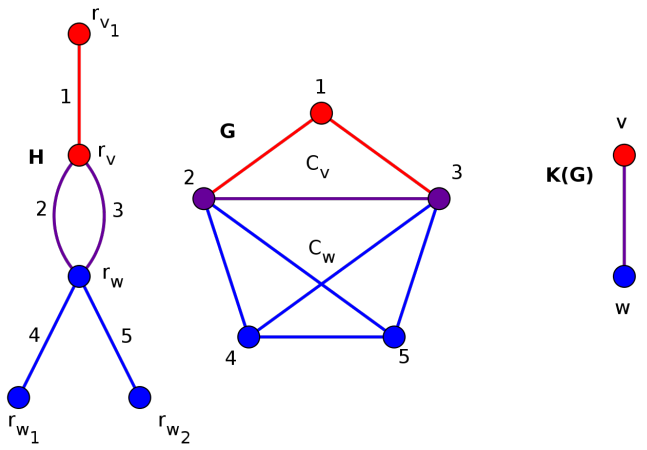

Figure 8 – Root graph H, line graph $G = L(H)$ and clique graph $K(G)$

Figure 8 depicts an example so that $K(L(H))$ is the reduced subgraph of H. Furthermore, it serves as an example of Algorithm 1, so that given G and $K(G)$, H is the output. In order to obtain H in this example, we start by setting H as a copy of $K(G)$. There are two vertices r_v and r_w. We look at G and count the number of vertices in the intersection of cliques C_v and C_w. In this case, we have two purple vertices (vertices 2 and 3). In H, we have the vertices associated with their respective maximal cliques linked by purple 2-multiedge, which corresponds to the two purple vertices. Now, we proceed by considering the other vertices, that is, the vertices that are in only one maximal clique. The up-hand maximal clique of G has only one extra red vertex (vertex 1). This vertex generates a new vertex in H (vertex r_{v_1}) and a new red edge in H linking the vertex r_v with the new vertex r_{v_1}. Similarly, we associate the two blue vertices (vertices 4 and 5) of the bottom-hand maximal clique with two edges (4 and 5) in H linking vertex $r_w \in H$ with r_{w_1} and r_{w_2}.

The Algorithm 1 works because we have supposed that $K(G)$ is triangle-free. Thus there is no vertex of G belonging to three maximal cliques otherwise the corresponding vertices of $K(G)$ would generate a triangle. The graph G cannot have a vertex in three

maximal cliques because this vertex would be associated with at least three edges in Step 1 of Algorithm 1. Thus we associate each vertex of G with one edge of H. Now we show that two vertices of G are adjacent if and only if their respective edges are adjacent in H. Two vertices are adjacent in G if and only if they are in the same maximal clique C_v if and only if their corresponding edges are adjacent, because these edges are incident to v. Therefore G is the line graph of H.

Theorem 2.2.5 *A graph G is the line graph of a triangle-free multigraph if and only if $K(G)$ is triangle-free.*

Proof Let G be the line graph of a triangle-free multigraph H. We initially assume G is connected. If H has only two vertices then G is a complete graph, so $K(G)$ has only one vertex and is triangle-free. If H has at least three vertices, by Lemma 2.4, $K(G)$ is the reduced subgraph of H thus it is triangle-free. If G is disconnected, we can apply the previous argument for each connected component.

Let G be a graph with $K(G)$ triangle-free, so we can use Algorithm 1 to return H (the root graph of G). Therefore G is the line graph of H. H is triangle-free because it is constructed by adding edges where already there are edges and with vertex of degree 1. □

Next theorem has already been proved by Peterson (PETERSON, 2003). Here we give an alternative simpler proof.

Theorem 2.2.6 *Let G be a graph. G is the line graph of a bipartite multigraph if and only if $K(G)$ is bipartite.*

Proof Let G be the line graph of a bipartite multigraph H. We initially assume G is connected. If H has only two vertices then G is a complete graph, so $K(G)$ has only one vertex and is bipartite. If H has at least three vertices, by Lemma 2.4, $K(G)$ is the reduced subgraph of H thus it is bipartite. If G is disconnected, we can apply the previous reasoning for each connected component.

Let G be a graph with $K(G)$ bipartide, so we can use Algorithm 1 to return H(the root graph of G). Therefore G is the line graph of H. H is bipartite because we can use the bipartition of $K(G)$ to distribute the vertices of H, each vertex of degree 1 are in the other partition of its adjacent vertex. □

Figure 9 shows that a graph G (right-hand graph) can have two different root multigraphs H_1 and H_2, that is, $L(H_1) = L(H_2) = G$. Note that the two previous theorems establish that there is a triangle-free and a bipartite root multigraph.

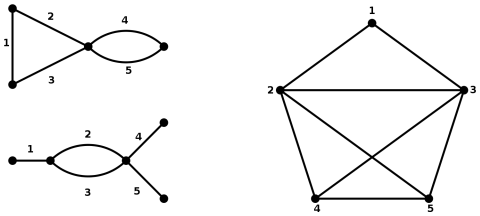

Figure 9 – The two multigraphs on the left are root graphs of the graph on the right.

Theorems 2.2.1, 2.2.2, and 2.2.6 can be summarized and form the following characterization of 2-tessellable graphs:

Theorem 2.2.7 *Let G be a graph, the following statements are equivalent:*
(a) G is 2-tessellable.
(b) $K(G)$ is bipartite.
(c) G is the line graph of a bipartite multigraph.
(d) G is β-free.

3 Coined walks

The classical random walks have applications to many fields as computer science, physics, chemistry, biology, and economics. The simplest example is a walker on the discrete line, he can move to the left or to the right. He tosses a coin and if it is tails he goes leftward if it is head he goes rightward. He repeats this processes indefinitely. The position of the walker is not deterministic, but we can calculate the probability that the walker is on the position d at time t. We can generalize this idea for a generic graph. The walker walks in the graph randomly, he can go only to a neighboring vertex. In quantum walk the dynamic is given by a unitary operator that can move the particle in the graph deterministically. Quantum mechanics gives us a superposition of the particle in many vertices. After a measure, we obtain the position of the particle probabilistically. In this chapter we present classical random walks and quantum walks with coins. You can find a more concise exposition in the article (KEMPE, 2003) and a more one in the book (PORTUGAL, 2013).

3.1 Classical random walk

In this section, we introduce the classical random walk on the line and on a general graph.

3.1.1 Random walk on the line

First we analyze the random walk on the line. Consider a particle walking along an axis of $\mathbb{Z}$. This particle begins in position 0 and in each step (or time) it goes one unit to the left with probability $1/2$ or one unit to the right with probability $1/2$. We can imagine that a non-biased coin is tossed and if it is heads the particle goes to left and if it is tails the particle goes to the right. We cannot predict the position of the particle at a certain time $t \neq 0$, but we can find the probability that the particle is on position n at time t (denoted by $p(n,t)$). For example the probability that the particle is on position -1 and 1 at time 1 is $1/2$ and $1/2$, that is, $p(-1,1) = p(1,1) = 1/2$. We assume that the particle cannot stand still at any step, so $p(0,1) = 0$, this is expected because for a fixed time t_0, the function $p(n,t_0)$ is a probability distribution, so

$$\sum_{n=-\infty}^{\infty} p(n,t_0) = 1,$$

for any t_0. Proceeding in this way we can verify the values of the table 1 which shows $p(n,t)$ given t and n (the empty cells represent probability 0). Note that the particle at time t cannot reach position n such that $|n| > t$.

t \ n	-5	-4	-3	-2	-1	0	1	2	3	4	5
0						1					
1					1/2		1/2				
2				1/4		1/2		1/4			
3			1/8		3/8		3/8		1/8		
4		1/16		1/4		3/8		1/4		1/16	
5	1/32		5/32		5/16		5/16		5/32		1/32

Table 1 – $p(n,t)$ given n and t.

Lemma 3.1.1 *The expression of $p(n,t)$ is given by*

$$p(n,t) = \begin{cases} 0, & \text{if } |n| > t \text{ or } t+n = 2k+1, k \in \mathbb{Z}; \\ \dfrac{1}{2^t}\begin{pmatrix} t \\ \frac{t+n}{2} \end{pmatrix}, & \text{otherwise.} \end{cases} \tag{3.1}$$

Proof At time t the farthest the particle can reach is the position $-t$ or t, so if $|n| > t$ then $p(n,t) = 0$.

We prove now that if $t+n$ is odd then $p(n,t) = 0$ by induction in t. Note that prove this argument proves that if the particle is situated on position n at time t then n and t have the same parity. For $t = 0$ only $p(0,0) \neq 0$. So if $t+n$ is odd then $p(n,t) = 0$. We are going to separate the inductive step in two, t_0 even and t_0 odd. For t_0 even, suppose that the particle is on an even position, so in the next step it will be on an odd position with time odd too. An analogous argument proves the result for t_0 odd.

In order to prove the formula for the nonzero values of $p(n,t)$ we observe first that, at time t, we have 2^t possibilities of different random walks, because in each step we have 2 possibilities. We define $l(n,t)$ and $r(n,t)$ as the number of steps the particle goes to left and right, respectively, to be situated on the position n at time t. We have that

$$\begin{cases} l(n,t) + r(n,t) = t \\ r(n,t) - l(n,t) = n \end{cases} \implies \begin{cases} r(n,t) = \dfrac{n+t}{2} \\ l(n,t) = \dfrac{t-n}{2} \end{cases}.$$

Note that if we know t and $r(n,t)$ then the position of particle is determined. We will calculate in how many ways we can go $r(n,t)$ steps to the right in time t. In other words, how many subsets of size $r(n,t)$ the set $\{\rightarrow_0, ..., \rightarrow_{t-1}\}$ possesses, where $\rightarrow_i$ represents the movement of the particle to the right at time i. Therefore if $t+n$ is even and $|n| < t$ we obtain

$$p(n,t) = \frac{1}{2^t}\begin{pmatrix} t \\ r(n,t) \end{pmatrix} = \frac{1}{2^t}\begin{pmatrix} t \\ \frac{t+n}{2} \end{pmatrix}. \qquad \square$$

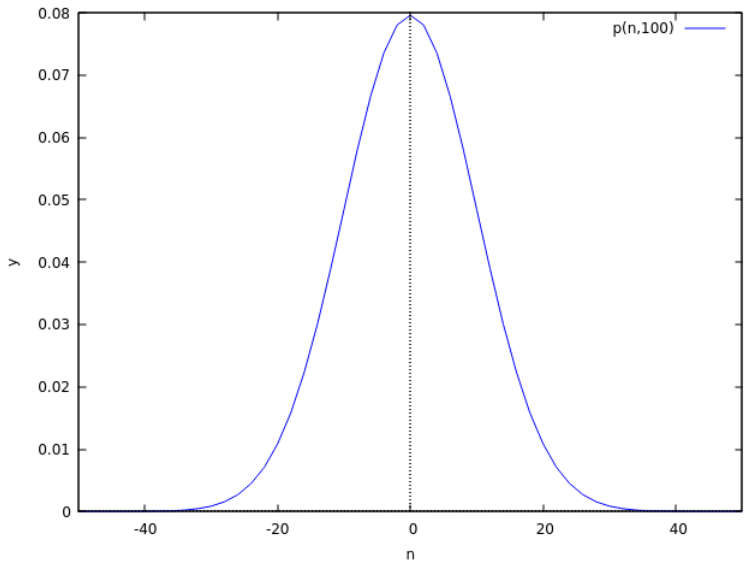

Figure 10 – The graph of $p(n, 100)$ without the zero entries.

With the previous lemma we can calculate the $p(n, t)$ for any n and t. In Figure 10 we show the graph of $p(n, 100)$ without the zero entries.

We are interested in estimating how far from the origin the particle is situated at time t. To do this we use the expected distance, which is a statistical quantity. The previous lemma is important because with it we can calculate the standard deviation of the random walk, which is equal to the expected distance when the probability distribution is symmetrical (note that $p(n, t) = p(-n, t)$ by equation (3.1)).

Proposition 3.1.2 *The standard deviation of the probability distribution at time t is*

$$\sigma(t) = \sqrt{t}. \tag{3.2}$$

Proof The standard deviation is given by $\sigma(t) = \sqrt{\langle n^2 \rangle - \langle n \rangle^2}$, where $\langle n^i \rangle$ is the i-th moment of the distance. Note that $p(n, t) = p(-n, t)$, so we have that

$$\langle n \rangle = \sum_{n=-\infty}^{\infty} np(n, t) = 0 \implies \sigma(t) = \sqrt{\sum_{-\infty}^{\infty} n^2 p(n, t)}. \tag{3.3}$$

Since $p(n, t) = 0$ when $|n| > t$ we have that

$$\sum_{-\infty}^{\infty} n^2 p(n, t) = \sum_{-t}^{t} n^2 p(n, t). \tag{3.4}$$

Using the change of variables $n = i - t$, the fact of $i = t + n$ odd implies $p(n, t) = 0$, the new change of variables $i = 2j$ and equation (3.1) we obtain the left-hand side of the following equation

$$\sum_{j=0}^{t} (2j - t)^2 \frac{1}{2^t} \binom{t}{j} = \frac{4}{2^t} \sum_{j=0}^{t} j^2 \binom{t}{j} - \frac{4t}{2^t} \sum_{j=0}^{t} j \binom{t}{j} + \frac{t^2}{2^t} \sum_{j=0}^{t} \binom{t}{j}.$$

Using the formulas

$$\sum_{k=0}^{m} k^2 \binom{m}{k} = m^2 2^{m-2} + m2^{m-2},$$

$$\sum_{k=0}^{m} k \binom{m}{k} = m2^{m-1} \text{ and } \sum_{k=0}^{m} \binom{m}{k} = 2^m$$

the right-hand side of the previous equation becomes, after some simplifications,

$$\sum_{-\infty}^{\infty} n^2 p(n,t) = t \tag{3.5}$$

and with the conclusion of the statement (3.3) we finalize the demonstration. □

3.1.2 Random walks on graphs

We use Markov chains to define a random walk on a graph G with n vertices. A Markov chain is a stochastic process, where we have the time $t \in \mathbb{N}$ (on the discrete-time case) and the state $p(t) \in [0,1]^n$, which is a probability distribution of the random walk at time t, that is, $p_i(t)$ is the probability of the particle being situated on vertex i at time t, so the sum of all $p_i(t)$ is equal to 1 for each time t fixed. The state is a function of time because it changes during the evolution of the system. We start with an initial state $p(0)$ and in each step we apply a matrix M, called of transition matrix (or probability matrix), that changes the probability distribution. So we have that

$$p(t) = M^t p(0), \tag{3.6}$$

note that M^t is not the transpose of M.

When the particle is in the vertex j it has probability M_{ij} to go for the vertex i, where M_{ij} is the entry of the transition matrix on the i-th row and j-th column. So M should satisfy two properties: i) all of its entries should be positive and ii) the sum of the entries of each column should be 1. These properties are sufficient to ensure that $p(t)$ is a probability distribution for all t. Indeed, if these properties hold, then

$$\sum_{i=1}^{n} p_i(t) = \sum_{i=1}^{n}\sum_{j=1}^{n} M_{ij} p_j(t-1) = \sum_{j=1}^{n}\sum_{i=1}^{n} M_{ij} p_j(t-1) = \sum_{j=1}^{n} p_j(t-1). \tag{3.7}$$

Since $p(0)$ is a probability distribution the result holds by induction.

It is common to define

$$M_{ij} = \begin{cases} 1/d_j, & \text{if } i \text{ is adjacent to } j, \\ 0, & \text{otherwise,} \end{cases} \tag{3.8}$$

where d_j is the degree of the vertex j. In this case we have that $M_{ij} = A_{ij}/d_j$, where A_{ij} is the entry of the adjacency matrix of the graph. We have that the particle only can go

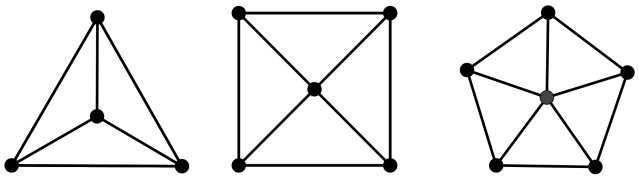

Figure 11 – The 3-wheel, 4-wheel and 5-wheel graphs.

to adjacent vertices and if it is in the vertex i it goes to the neighbors of i with the same probability. We call this as uniform random walk.

We take as an example the uniform random walk on the n-wheel graph. Figure 11 shows the 3-wheel, 4-wheel, and 5-wheel. We label the vertices of the graph so that $1, \ldots, n$ are the vertices of the cycle and $n+1$ is the central vertex. Hence, the transition matrix of this graph is given by

$$M = \begin{bmatrix} 0 & \frac{1}{3} & 0 & \ldots & \frac{1}{3} & \frac{1}{n} \\ \frac{1}{3} & 0 & \frac{1}{3} & \ldots & 0 & \frac{1}{n} \\ 0 & \frac{1}{3} & 0 & \ldots & 0 & \frac{1}{n} \\ \vdots & \vdots & \vdots & \ddots & \vdots & \vdots \\ \frac{1}{3} & 0 & 0 & \ldots & 0 & \frac{1}{n} \\ \frac{1}{3} & \frac{1}{3} & \frac{1}{3} & \ldots & \frac{1}{3} & 0 \end{bmatrix}.$$

Note that each vertex of the cycle has 3 neighbors and the central vertex has n neighbors.

We assume as initial condition that the particle is in the central vertex. So we have that

$$p(0) = \begin{bmatrix} 0 \\ \vdots \\ 0 \\ 1 \end{bmatrix}.$$

Proposition 3.1.3 *The probability distribution at time t is given by*

$$p(t) = \begin{bmatrix} f_n(t) \\ f_n(t) \\ \vdots \\ f_n(t) \\ g_n(t) \end{bmatrix}, \tag{3.9}$$

where $f_n(t) = \dfrac{3^t - (-1)^t}{4n3^{t-1}}$ *and* $g_n(t) = \dfrac{3^{t-1} - (-1)^{t-1}}{4 \cdot 3^{t-1}}$.

Proof We prove by induction on t. We can verify that equation (3.9) holds for $p(0)$. We suppose that it holds for $p(t)$. Note that

$$p(t+1) = Mp(t) = M \begin{bmatrix} f_n(t) \\ \vdots \\ g_n(t) \end{bmatrix} =$$

$$\begin{bmatrix} \frac{2 \cdot (3^t - (-1)^t)}{3 \cdot 4n3^{t-1}} + \frac{3^{t-1} - (-1)^{t-1}}{4n3^{t-1}} \\ \vdots \\ \frac{n(3^t - (-1)^t)}{3 \cdot 4n3^{t-1}} \end{bmatrix} = \begin{bmatrix} \frac{3^{t+1} - (-1)^{t+1}}{4n3^t} \\ \vdots \\ \frac{3^t - (-1)^t}{4 \cdot 3^t} \end{bmatrix}$$

is the inductive step. □

Analyzing the expression of $p(t)$ we can see as t tends to infinity the probability of the particle being situated in the central vertex tends to $1/4$ and that of a vertex of the cycle tends to $3/4n$.

3.2 Discrete-time quantum walk

In this section, we introduce the coined quantum walk on the line and on a general graph.

3.2.1 Quantum walk on the line

Discrete-time quantum walks are the quantum version of discrete-time classical random walks. To compare with the classical case we start studying the quantum walk on the line using the coined model. We associate the position of the particle with a Hilbert space $\mathcal{H}_p$ (position space) which has as one possible basis the set $\left\{\left|i\right\rangle; i \in \mathbb{Z}\right\}$. We need one more Hilbert space $\mathcal{H}_c$ (coined space) which is associated with the spin of the particle. If we have a spin up we associate it with the vector $\left|\uparrow\right\rangle$ and if we have a spin down we associate it with the vector $\left|\downarrow\right\rangle$. These two vectors (coin vectors) form a basis of $\mathcal{H}_c$ and report if the particle goes leftward or rightward. Suppose the particle is situated on position $\left|n\right\rangle$, if it has spin up then in the next step it goes to position $\left|n+1\right\rangle$ and if it has spin down it goes to position $\left|n-1\right\rangle$. Finally, we define the Hilbert space $\mathcal{H} = \mathcal{H}_c \otimes \mathcal{H}_p$ where the quantum walk act.

We are interested in two evolution operators, one is the coin operator C, which can transform the coin vector on a coin, and other is the shift operator S, which makes the particle walk through the line. As aforementioned the shift operator should satisfy

$$S\left|\uparrow\right\rangle\left|n\right\rangle = \left|\uparrow\right\rangle\left|n+1\right\rangle,$$
$$S\left|\downarrow\right\rangle\left|n\right\rangle = \left|\downarrow\right\rangle\left|n-1\right\rangle.$$

We can verify that

$$S = \Big|\downarrow\Big\rangle\Big\langle\downarrow\Big| \sum_{n=-\infty}^{\infty} \Big|n-1\Big\rangle\Big\langle n\Big| + \Big|\uparrow\Big\rangle\Big\langle\uparrow\Big| \sum_{n=-\infty}^{\infty} \Big|n+1\Big\rangle\Big\langle n\Big|. \tag{3.10}$$

We can choose several linear transformations for the coin operator. Let $\Big|\psi(0)\Big\rangle = \Big|\uparrow\Big\rangle\Big|0\Big\rangle$ be the initial state of the quantum walk. If we apply the shift operator recurrently in $\Big|\psi(0)\Big\rangle$ the particle goes to the right in all steps, for this reason we need the coin operator. We use as coin operator the Hadamard operator

$$H = \frac{1}{\sqrt{2}}\left(\Big|\uparrow\Big\rangle\Big\langle\uparrow\Big| + \Big|\uparrow\Big\rangle\Big\langle\downarrow\Big| + \Big|\downarrow\Big\rangle\Big\langle\uparrow\Big| - \Big|\downarrow\Big\rangle\Big\langle\downarrow\Big|\right), \tag{3.11}$$

which generates an unbiased coin. Now we define the evolution operator as $U = S \cdot (H \otimes I)$, which plays a central role on the quantum walk. Now if we apply U to the initial state we obtain

$$U\Big|\psi(0)\Big\rangle = \frac{1}{\sqrt{2}}\left(\Big|\downarrow\Big\rangle\Big|-1\Big\rangle + \Big|\uparrow\Big\rangle\Big|1\Big\rangle\right). \tag{3.12}$$

If we make a measurement, on the last state, using the standard basis, we get $\Big|\downarrow\Big\rangle\Big|-1\Big\rangle$ with probability 1/2 and $\Big|\uparrow\Big\rangle\Big|1\Big\rangle$ with probability 1/2 too. If we repeat this process (take the resulting state, applying U and making a measurement), we obtain the classical random walk on the line exactly as studied on subsection 3.1.1.

t \ n	-5	-4	-3	-2	-1	0	1	2	3	4	5
0						1					
1					1/2		1/2				
2				1/4		1/2		1/4			
3			1/8		1/8		5/8		1/8		
4		1/16		1/8		1/8		5/8		1/16	
5	1/32		5/32		1/8		1/8		17/32		1/32

Table 2 – Table of $p_n(t)$ given n and t.

The point of the quantum walk is not to make intermediary measurements to better explore quantum superposition and interference. The idea here is to apply U a determined number of times to the initial state and only after this make a measurement. Each step of the quantum walk is the application of U to the previous state, that is, $\Big|\psi(t)\Big\rangle = U\Big|\psi(t-1)\Big\rangle$, where $\Big|\psi(t)\Big\rangle$ is the state of the quantum walk on step t. Explicitly, we have that

$$\Big|\psi(t)\Big\rangle = U^t\Big|\psi(0)\Big\rangle. \tag{3.13}$$

Computing the first three steps of the quantum walk illustrates a difference with the classical world,

$$\begin{aligned}
\big|\psi(1)\big\rangle &= U\big|\psi(0)\big\rangle = \frac{1}{\sqrt{2}}\left(\big|\downarrow\big\rangle\big|-1\big\rangle + \big|\uparrow\big\rangle\big|1\big\rangle\right),\\
\big|\psi(2)\big\rangle &= U\big|\psi(1)\big\rangle = \frac{1}{2}\left(-\big|\downarrow\big\rangle\big|-2\big\rangle + \big|\uparrow\big\rangle\big|0\big\rangle + \big|\downarrow\big\rangle\big|0\big\rangle + \big|\uparrow\big\rangle\big|2\big\rangle\right),\\
\big|\psi(3)\big\rangle &= U\big|\psi(2)\big\rangle = \frac{1}{2\sqrt{2}}\left(\big|\downarrow\big\rangle\big|-3\big\rangle - \big|\uparrow\big\rangle\big|-1\big\rangle + \big|\downarrow\big\rangle\big|1\big\rangle + 2\big|\uparrow\big\rangle\big|1\big\rangle + \big|\uparrow\big\rangle\big|3\big\rangle\right).
\end{aligned}$$

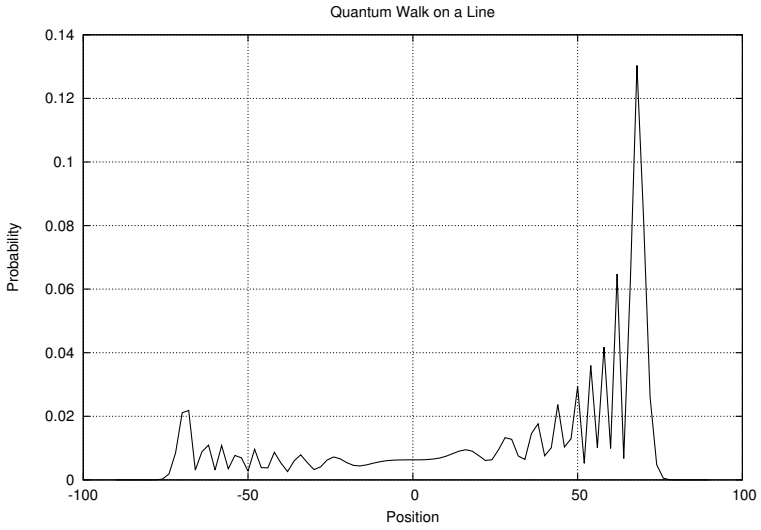

Figure 12 – Graph of the probability distribution after the measurement on the step 100 with initial state $\big|\psi(0)\big\rangle = \big|\uparrow\big\rangle\big|0\big\rangle$.

The probability of finding the particle on position n after t steps is given by

$$p_n(t) = \Big|\big\langle\psi(t)\big|\left(\big|\uparrow\big\rangle\big|n\big\rangle\right)\Big|^2 + \Big|\big\langle\psi(t)\big|\left(\big|\downarrow\big\rangle\big|n\big\rangle\right)\Big|^2.$$

For a fixed t, $p_n(t)$ is a probability distribution. If we measure after the first and second steps we obtain the same distribution of the classical random walk on the line, but if the measurement is performed after the third step a different distribution holds. Table 2 shows the probability distribution of the quantum walk on the line after t steps, which displays a remarkable difference when compared to Table 1. Such difference is due to quantum interference, which is firstly seen when $\big|\psi(3)\big\rangle$ is computed, the terms with $\big|-1\big\rangle$ take a destructive interference and the terms with $\big|1\big\rangle$ take a constructive. In Figure 12 we see the probability distribution if the measurement is realized on step 100 of such quantum walk, again the particle is concentrated with larger probability on the right. This concentration is due to the initial state's choice, but if a different one is considered, $\big|\psi(0)\big\rangle = \big|\downarrow\big\rangle\big|0\big\rangle$, in step 100 we would get the symmetrical graph of the Figure 12. To get a symmetrical probability distribution we have to take as initial state a linear combination of the two states of the coin, for example consider

$$\big|\psi(0)\big\rangle = \frac{1}{\sqrt{2}}\left(\big|\uparrow\big\rangle + i\big|\downarrow\big\rangle\right)\big|0\big\rangle.$$

Note that since Hadamard operator does not have complex entries, the trajectories of $\left|\uparrow\right\rangle$ and $\left|\downarrow\right\rangle$ have no interference with each other. Figure 13 shows the probability distribution of this quantum walk with the above initial state if we measure in the 100-th step. Figures 12 and 13 were generated using the program Hiperwalk[1].

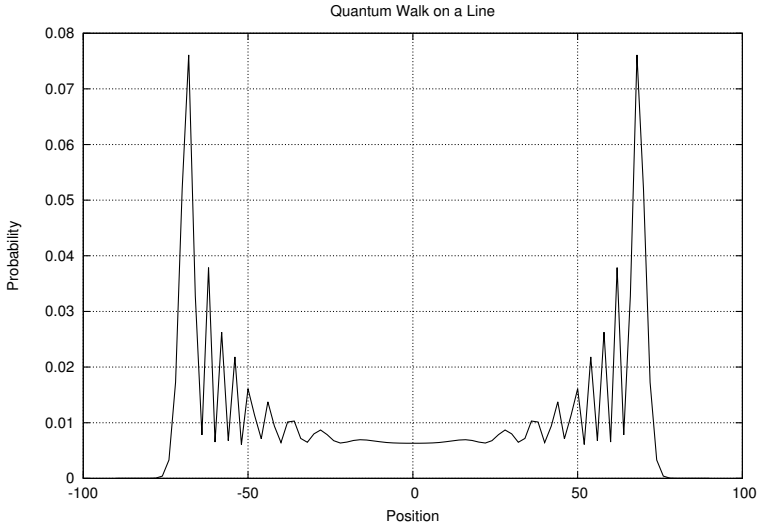

Figure 13 – Graph of the probability distribution after the measurement on the step 100 with initial state $\left|\psi(0)\right\rangle = \frac{1}{\sqrt{2}}\left(\left|\uparrow\right\rangle\left|0\right\rangle + i\left|\downarrow\right\rangle\left|0\right\rangle\right)$.

In subsection 3.1.1, we saw that the standard deviation of the classical random walk on the line is $\sqrt{t}$. We want to compare this with the quantum case. When we simulate the quantum walk on Hiperwalk it returns the standard deviation for different values of the time. In Figure 14 we have a comparison of the standard deviation in the two cases and we have that $\sigma(t) = 0.54t$ in the second case. The fact that we have a linear dependence on the standard deviation is remarkable. If the particle has a deterministic walk, let us say it goes to the right in each step the standard deviation would be exactly t, that is, a linear dependence too. We say that the movement has a ballistic behavior. We also have this behavior for the quantum walk with approximately half of the velocity, with the advantage that the particle can be situated in the two sides of the line.

3.2.2 Quantum walk on graphs

Now we define the coined quantum walk on general graphs. We begin with a d-regular graph, that is, a graph such that each vertex has degree d. In this case we denote, for each vertex v, the edges that links v with others vertices by e_v^j, with $j \in \{1, ..., d\}$. As we can see in Figure 15 the labels of the edges are determined by the vertex that edge links (note that the two labels of the same edge are entirely independent). The Hilbert

[1] HiperWalk is a freeware open-source program that allows the user to perform simulations of quantum walks on graphs using HPC.

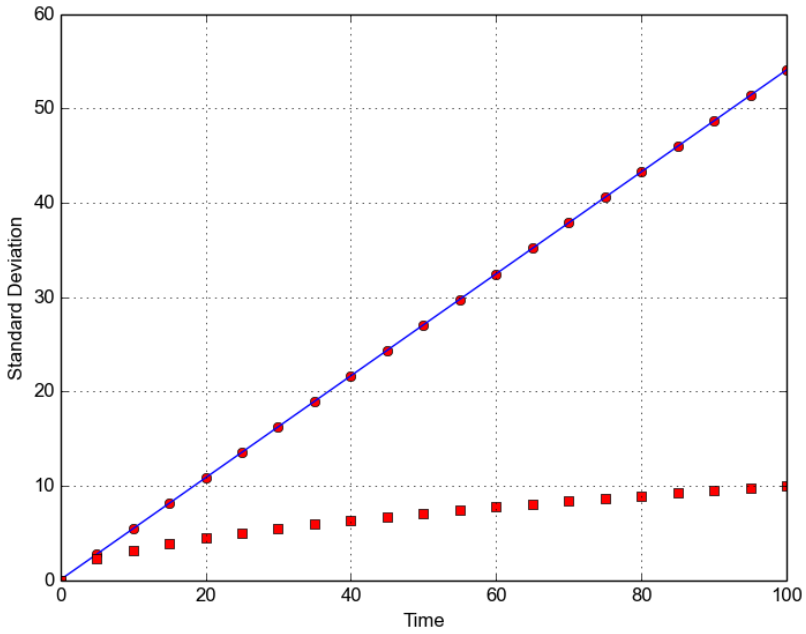

Figure 14 – Graph of the standard deviation of the random walk (squares) and quantum walk (circles) on the line.

space $\mathcal{H}_c$ of the coin has dimension d. The shift operator is defined by

$$S\big|j\big\rangle\big|v\big\rangle = \begin{cases} \big|j\big\rangle\big|w\big\rangle, \text{ if } e_v^j = vw \\ 0, \text{ otherwise.} \end{cases} \tag{3.14}$$

If we want to maintain the property that the coin is balanced, that is, the particle has the same probability to go to a neighboring vertex, we can use the generalization of the Hadamard operator, the Discrete Fourier Transform defined as

$$DFT = \frac{1}{\sqrt{d}} \begin{bmatrix} 1 & 1 & 1 & \dots & 1 \\ 1 & w & w^2 & \dots & w^{d-1} \\ \vdots & \vdots & \vdots & \ddots & \vdots \\ 1 & w^{d-1} & w^{2(d-1)} & \dots & w^{(d-1)(d-1)} \end{bmatrix},$$

where $w = \exp\left(\frac{2\pi i}{d}\right)$ is a d-th root of unity.

If the graph is not d-regular, we can define the quantum walk in many ways. Let d be the largest degree of the graph vertices. On each vertex we add loops (an edge that links a vertex with itself) until the graph becomes d-regular (each loop adds 1 to the degree of the vertex), as we can see in Figure 16. Therefore we get a d-regular graph and the coined quantum walk can now be defined. Another way to define a quantum walk with coin is to define a coin operator for each vertex of the graph.

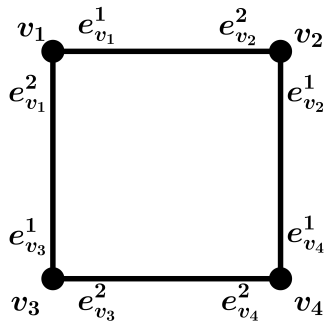

Figure 15 – A 2-regular graph with labels, for the edges and vertices.

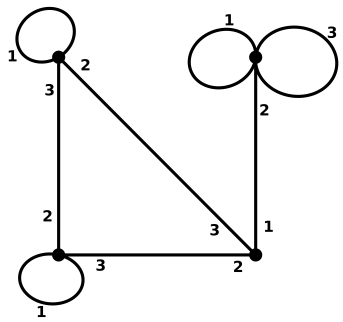

Figure 16 – A graph with the loops completing the degree of the vertices of the graph.

4 Staggered Quantum Walk

We can define a quantum walk without the use of a coin. This is useful for various reasons, the main one being that it allow us to use a Hilbert space of smaller dimension. There were more than one model of coinless quantum walk. In this section, we focus on a recently proposed model, the staggered quantum walk (SQW) (PORTUGAL et al., 2016).

Let $G(V, E)$ be a 2-tessellable graph with vertex set $V(G)$ and edge set $E(G)$. Let $\mathcal{T}_\alpha, \mathcal{T}_\beta$ be tessellations that cover all edges of G. Let $\mathcal{T}_\alpha = \{\alpha_0, ..., \alpha_{n_0-1}\}$ be the first graph tessellation with n_0 polygons and let $\mathcal{T}_\beta = \{\beta_0, ..., \beta_{n_1-1}\}$ be the second graph tessellation with n_1 polygons. We take as Hilbert space $\mathcal{H}^m$, where $m = |V(G)|$ can be infinite. The computational basis of this Hilbert space is $\left\{\left|k\right\rangle, k \in V(G)\right\}$, that is, we associate each vertex of the graph with a state of the computational basis. Three steps are required to construct the staggered quantum walk.

First, we associate each polygon α_j of the tessellation $\mathcal{T}_\alpha$ with a unit vector $\left|\alpha_j\right\rangle$ in such a way that

$$\left|\alpha_j\right\rangle = \sum_{k \in V(G)} a_{j,k} \left|k\right\rangle, \tag{4.1}$$

where $a_{jk} \in \mathbb{C}$ with $a_{j,k} \neq 0$ if $k \in \alpha_j$ and $a_{j,k} = 0$ otherwise. The most usual amplitudes are the uniform distribuition, that is, $a_{j,k} = 1/\sqrt{|\alpha_j|}$ if $k \in \alpha_j$. We make this association to the polygons of the tessellation $\mathcal{T}_\beta$ too. We have that

$$\left|\beta_j\right\rangle = \sum_{k \in V(G)} b_{j,k} \left|k\right\rangle, \tag{4.2}$$

where $b_{j,k} \neq 0$ if $k \in \beta_j$ and $b_{j,k} = 0$ otherwise.

Second, we define two local operators. A local operator is an operator that preserves the structure of the graph, that is, if the particle is in vertex v then the application of this operator takes the particle only to a neighbor of v. They are defined as

$$H_0 = 2 \sum_{j=0}^{n_0-1} \left|\alpha_j\right\rangle\left\langle\alpha_j\right| - I, \tag{4.3}$$

$$H_1 = 2 \sum_{j=0}^{n_1-1} \left|\beta_j\right\rangle\left\langle\beta_j\right| - I. \tag{4.4}$$

We prove that H_0 is unitary and Hermitian, that is, $H_0^2 = I$. Using the fact that $\left\langle\alpha_j\middle|\alpha_{j'}\right\rangle = \delta_{jj'}$ we have that

$$\begin{aligned} H_0^2 = \; & 4 \sum_{j=0}^{n_0-1} \sum_{j'=0}^{n_0-1} \left|\alpha_j\right\rangle\left\langle\alpha_j\middle|\alpha_{j'}\right\rangle\left\langle\alpha_{j'}\right| - 2 \sum_{j=0}^{n_0-1} \left|\alpha_j\right\rangle\left\langle\alpha_j\right| - 2 \sum_{j'=0}^{n_0-1} \left|\alpha_{j'}\right\rangle\left\langle\alpha_{j'}\right| + I = \\ & 4 \sum_{j=0}^{n_0-1} \left|\alpha_j\right\rangle\left\langle\alpha_j\right| - 4 \sum_{j=0}^{n_0-1} \left|\alpha_j\right\rangle\left\langle\alpha_j\right| + I = I \end{aligned}$$

Analogously, we prove that H_1 is unitary and Hermitian. Therefore H_0 and H_1 are reflections.

Third, we define the evolution operator as (PORTUGAL; OLIVEIRA; MOQADAM, 2017)

$$U = e^{i\theta_1 H_1} e^{i\theta_0 H_0}. \tag{4.5}$$

We must pay attention to two important factors. First, equations (4.3) and (4.4) are defined in such a way that the particle situated on a vertex of a polygon only moves to vertices in this polygon. Since the polygon is a clique, the operators H_0 and H_1 are local. Second, if two tessellations do not cover all edges, we have to define more tessellations until all edges are covered, because if there is an edge E that is not covered by any tessellation the staggered quantum walk would have the same dynamic with and without E. To each new tessellation we associate a new local operator. In the next section, we see a more detailed example of the staggered quantum walk.

4.1 SQW on the line of diamonds

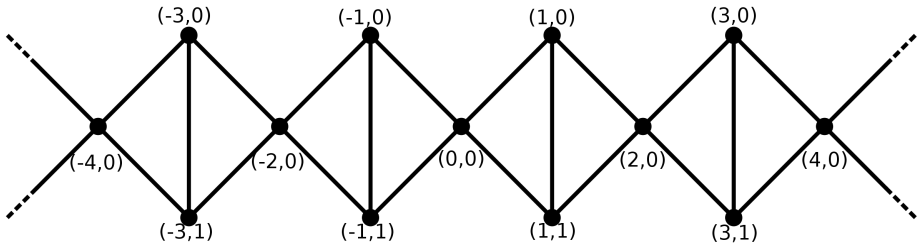

Figure 17 – Line of diamonds

A diamond is a complete graph with four vertices with one edge removed. The line of diamonds is a graph obtained by replacing each vertex of an infinite one-dimensional lattice by a diamond(Figure 17). In this graph we can describe the position of a particle in a vertex (x, y) by a unitary vector $\left|x, y\right\rangle$, where $x \in \mathbb{Z}$ is the horizontal position and $y \in \{0, 1\}$ is the vertical position. These vectors form an orthonormal basis of the Hilbert space $\mathcal{H}^{\infty}$ associated with this graph. A quantum walk is determined by its evolution operator. In the staggered quantum walk, the graph structure plays a key role. Since the particle can only move from a vertex to another if they are adjacent, the cliques of the graph induce how the particle moves. Remember that the set of edges of a graph can be partitioned by the set of maximal cliques.

The first thing we have to do is a partition of the set of vertices such that each element of the partition is a clique. We call the elements of the partition by polygon and the partition by tessellation. Figure 18 shows an example of a tessellation of the line of diamonds. Each polygon consists of the three vertices in the red triangle, and the

tessellation is the set of all triangles. An edge is covered by a polygon if the endpoints of the edge are in the polygon.

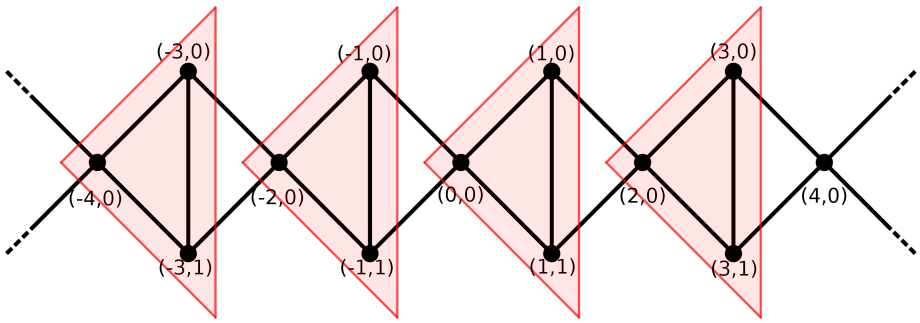

Figure 18 – Line of diamonds with red tessellation

Now we associate each polygon with a unit vector. To do this association the vectors that describe the vertices of the polygon should have non-zero complex amplitudes and all the others vectors should have amplitudes equal to zero. The most usual association is the uniform superposition

$$\left|u_x^0\right\rangle = \frac{1}{\sqrt{3}}\left(\left|2x,0\right\rangle + \left|2x+1,0\right\rangle + \left|2x+1,1\right\rangle\right).$$

The first local operator is

$$H_0 = 2\sum_{x=-\infty}^{\infty}\left|u_x^0\right\rangle\left\langle u_x^0\right| - I.$$

Let us check how it works if the particle is in vertex $(0,0)$:

$$\begin{aligned} H_0\left|0,0\right\rangle &= 2\sum_{x=-\infty}^{\infty}\left|u_x^0\right\rangle\left\langle u_x^0\right|0,0\right\rangle - \left|0,0\right\rangle \\ &= \frac{2}{\sqrt{3}}\sum_{x=-\infty}^{\infty}\left|u_x^0\right\rangle\delta_{x0} - \left|0,0\right\rangle \\ &= \frac{-1}{3}\left|0,0\right\rangle + \frac{2}{3}\left|1,0\right\rangle + \frac{2}{3}\left|1,1\right\rangle. \end{aligned}$$

We can see in Figure 18 that, after applying H_0, the particle is in the polygon that contains the vertex $(0,0)$. This property can be extended to any vector of the computational basis. This means that we need more operators for the particle to cross all the graph.

Thus we make a new tessellation as we can see in Figure 19. Similarly we associate each polygon with the unitary vector

$$\left|u_x^1\right\rangle = \frac{1}{\sqrt{3}}(\left|2x,0\right\rangle + \left|2x-1,0\right\rangle + \left|2x-1,1\right\rangle).$$

The second local operator is

$$H_1 = 2\sum_{x=-\infty}^{\infty}\left|u_x^1\right\rangle\left\langle u_x^1\right| - I.$$

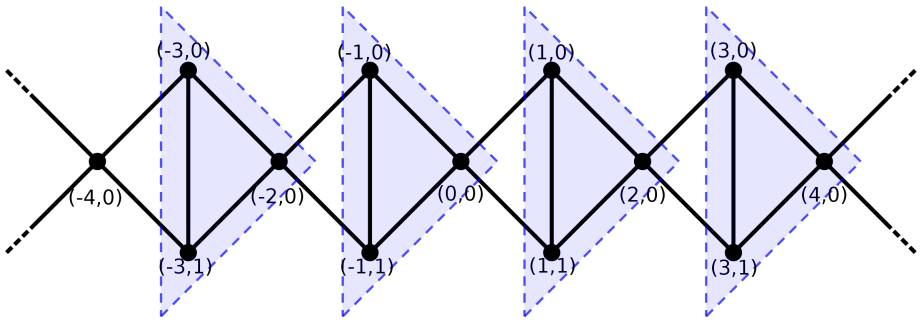

Figure 19 – Line of diamonds with blue tessellation

We do this until all the edges belong to at least one tessellation. In this way we cover all edges. The evolution operator is

$$U = e^{i\theta H_1} e^{i\theta H_0}$$

and the state in time t is

$$\left|\psi(t)\right\rangle = U^t \left|\psi(0)\right\rangle \tag{4.6}$$

where $\left|\psi(0)\right\rangle$ is the initial state. The probability of finding the walker on vertex (x, y) after t time steps is $p_{x,y}(t) = \left|\left\langle x, y \middle| \psi(t)\right\rangle\right|^2$. When we fix t, $p_{x,y}(t)$ is a probability distribution.

4.2 Simulation of the SQW on the line of diamonds

We want to determine the standard deviation of the position of the walker of the staggered quantum walk in the line of diamonds. With this information we can know how far the particle moves from the initial location $\left|\psi(0)\right\rangle = \left|0, 0\right\rangle$. We want to know with which θ we obtain a higher standard deviation. For this purpose, we use the program HiperWalk.[1]

To use Hiperwalk we provide $e^{i\theta H_1}$ and $e^{i\theta H_0}$ in matrix form. Remember that for any t the $\left|\psi(t)\right\rangle$ in computational basis has complex amplitude equal to 0 for an infinite number of vectors of the computational basis. A staggered quantum walk that does not reach the borders of a finite line of diamonds is also a walk in an infinite line of diamonds. So we can do the simulation for a sufficiently large number of vertices with a time which the walker does not reach the border. We choose 60,000 vertices(20,000 diamonds) and 10,000 time steps. Thus the input are two complex matrices 60000×60000, but they are highly sparse by construction. For the initial state, we take $\left|\psi(0)\right\rangle = \left|0, 0\right\rangle$. We choose as output the state $\left|\psi(10000)\right\rangle$ and the intermediary states $\left|\psi(1000k)\right\rangle$. Next we calculated the standard deviation for the staggered quantum walk when the steps time are multiples of 1000 to verify if we have a linear function as expected. Figure 20 plots the standard

[1] HiperWalk is a freeware open-source program that allows the user to perform simulations of quantum walks on graphs using HPC.

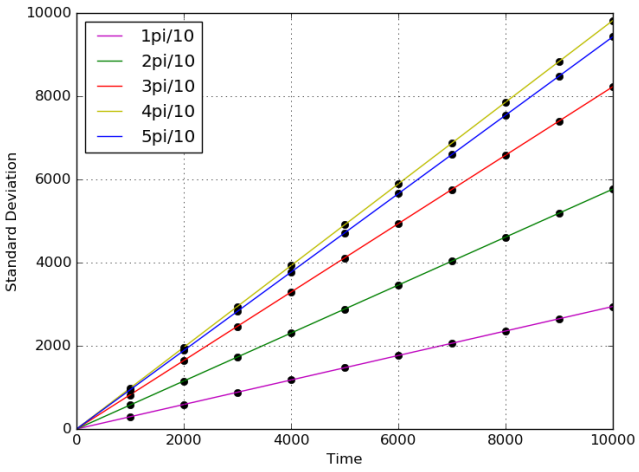

Figure 20 – Standard Deviation for $\theta = \pi/10, \pi/5, 3\pi/10, 2\pi/5$ and $\pi/2$

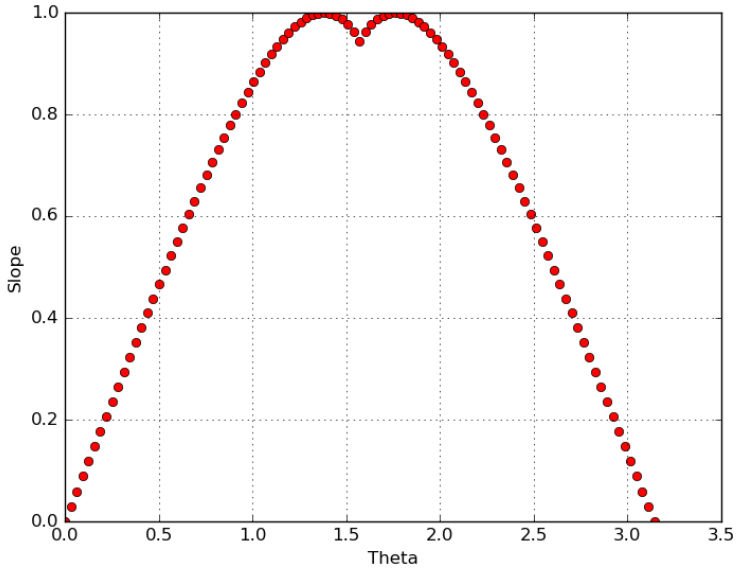

Figure 21 – Slope for different θ

deviation $\sigma(t)$ as a function of t for some values of θ. These results show that $\sigma(t)$ is a linear function of t, whose slope depends on θ.

Now we calculate the slope $\sigma(t)/t$ for various values of θ. Figure 21 shows $\sigma(t)/t$ as a function of $\theta \in \{i\pi/100; 0 \leq i \leq 100\}$. The largest slope is obtained for $\theta = 44\pi/100$ and $56\pi/100$. Since $\sigma(t)$ is a linear function of t, we have that the movement of the particle is ballistic.

4.3 Analysis of standard deviation

Now we are interested to find an expression for the standard deviation for a general θ. This expression comes from:

$$\sigma(t) = \sqrt{\langle \hat{D}^2 \rangle_t - \langle \hat{D} \rangle_t^2}, \tag{4.7}$$

where $\langle \hat{D}^n \rangle_t$ is the n-th moment of the distance at time t.

4.3.1 The n-th moment

To calculate analytically the standard deviation we use the symmetry of the graph. We can see that all the vertices of the form $(2x, 0)$ are symmetrical. The same holds for $(2x+1, 0)$ and $(2x+1, 1)$. So we can define a Fourier basis for the Hilbert space using the periodicity of the graph. We define the staggered Fourier basis (SANTOS; PORTUGAL; BOETTCHER, 2015) as:

$$\left|\psi_k^0\right\rangle = \sum_{x=-\infty}^{\infty} e^{-ik(2x)} \left|2x, 0\right\rangle$$

$$\left|\psi_k^1\right\rangle = \frac{1}{\sqrt{2}} \sum_{x=-\infty}^{\infty} e^{-ik(2x+1)} \left(\left|2x+1, 0\right\rangle + \left|2x+1, 1\right\rangle\right)$$

$$\left|\psi_k^2\right\rangle = \frac{1}{\sqrt{2}} \sum_{x=-\infty}^{\infty} e^{-ik(2x+1)} \left(\left|2x+1, 0\right\rangle - \left|2x+1, 1\right\rangle\right)$$ We can reduce these three equations to only one:

$$\left|\psi_k^p\right\rangle = \left(\frac{1}{\sqrt{2}}\right)^{1-\delta_{p0}} \sum_{x=-\infty}^{\infty} e^{-ik(2x+1-\delta_{p0})} \left(\left|2x+1-\delta_{p0}, 0\right\rangle + (\delta_{p0}-1)^{p+1}\left|2x+1, 1\right\rangle\right)$$

These vectors are very important in quantum walks because of the following statement and proposition.

Statement 4.3.1 *The set* $\left\{\left|\psi_k^p\right\rangle; 0 \leq p \leq 2, k \in (-\pi, \pi)\right\}$ *is formed by orthogonal vectors of the Hilbert space, that is,* $\left\langle \psi_k^p \middle| \psi_{k'}^{p'} \right\rangle = \delta_{pp'}\delta(k-k')$.

Before we see the next proposition, we denote by Ω_k the hyperplane spanned by $\left\{\left|\psi_k^0\right\rangle, \left|\psi_k^1\right\rangle, \left|\psi_k^2\right\rangle\right\}$ for a fixed k.

Proposition 4.3.2 *For a fixed* k, Ω_k *is invariant under the action of* H_0 *and* H_1, *that is,* $\left|u\right\rangle \in \Omega_k \implies H_0\left|u\right\rangle, H_1\left|u\right\rangle \in \Omega_k$.

Proof We are going to verify how H_0 and H_1 act on $\left|\psi_k^0\right\rangle$, $\left|\psi_k^1\right\rangle$ and $\left|\psi_k^2\right\rangle$.

$$\begin{aligned}
H_0\left|\psi_k^0\right\rangle &= \sum_{x=-\infty}^{\infty} e^{-ik2x} H_0\left|2x,0\right\rangle \\
&= \sum_{x=-\infty}^{\infty} e^{-ik2x}\left(-\frac{1}{3}\left|2x,0\right\rangle + \frac{2}{3}\left|2x+1,0\right\rangle + \frac{2}{3}\left|2x+1,1\right\rangle\right) \\
&= -\frac{1}{3}\sum_{x=-\infty}^{\infty} e^{-ik2x}\left|2x,0\right\rangle + \frac{2\sqrt{2}e^{ik}}{3}\left(\frac{1}{\sqrt{2}}\right)\sum_{x=-\infty}^{\infty} e^{-ik(2x+1)}\left(\left|2x+1,0\right\rangle + \left|2x+1,1\right\rangle\right) \\
&= -\frac{1}{3}\left|\psi_k^0\right\rangle + \frac{2\sqrt{2}e^{ik}}{3}\left|\psi_k^1\right\rangle
\end{aligned}$$

Similarly we obtain:

$H_0\left|\psi_k^1\right\rangle = +\frac{2\sqrt{2}e^{-ik}}{3}\left|\psi_k^0\right\rangle + \frac{1}{3}\left|\psi_k^1\right\rangle$

$H_0\left|\psi_k^2\right\rangle = -\left|\psi_k^2\right\rangle$

$H_1\left|\psi_k^0\right\rangle = -\frac{1}{3}\left|\psi_k^0\right\rangle + \frac{2\sqrt{2}e^{-ik}}{3}\left|\psi_k^1\right\rangle$

$H_1\left|\psi_k^1\right\rangle = +\frac{2\sqrt{2}e^{ik}}{3}\left|\psi_k^0\right\rangle + \frac{1}{3}\left|\psi_k^1\right\rangle$

$H_1\left|\psi_k^2\right\rangle = -\left|\psi_k^2\right\rangle$

A vector is in Ω_k if and only if it is a linear combination of $\left|\psi_k^0\right\rangle$, $\left|\psi_k^1\right\rangle$ and $\left|\psi_k^2\right\rangle$. For any vector $\left|u\right\rangle \in \Omega_k$, it is easy to verify, using the above equalities, that $H_0\left|u\right\rangle, H_1\left|u\right\rangle \in \Omega_k$. Therefore Ω_k is invariant under H_0 and H_1.□

The last proposition gives us, for a fixed k, two reduced matrices H_0^k and H_1^k which act on Ω_k, they are, respectively, H_0 and H_1 restricted to Ω_k in the basis $\left\{\left|\psi_k^0\right\rangle, \left|\psi_k^1\right\rangle, \left|\psi_k^2\right\rangle\right\}$. We have that

$$H_0^k = \begin{bmatrix} -\frac{1}{3} & \frac{2\sqrt{2}e^{-ki}}{3} & 0 \\ \frac{2\sqrt{2}e^{ki}}{3} & \frac{1}{3} & 0 \\ 0 & 0 & -1 \end{bmatrix}$$

and

$$H_1^k = \begin{bmatrix} -\frac{1}{3} & \frac{2\sqrt{2}e^{ki}}{3} & 0 \\ \frac{2\sqrt{2}e^{-ki}}{3} & \frac{1}{3} & 0 \\ 0 & 0 & -1 \end{bmatrix}$$

Consider an operador from $\mathcal{H}$ to Ω_k, which maps $\left|\psi_k^p\right\rangle$ to the 3-dimensional vector $\left|p\right\rangle$. We define H_0^k as H_0 restricted to Ω_k and consequently we obtain

$$H_0\left|\psi_k^p\right\rangle = \sum_{p'=0}^{2} \left\langle p'\right|H_0^k\left|p\right\rangle\left|\psi_k^{p'}\right\rangle, \tag{4.8}$$

Similarly H_1^k is H_1 restricted to Ω_k and then

$$H_1\left|\psi_k^p\right\rangle = \sum_{p'=0}^{2} \left\langle p'\right|H_1^k\left|p\right\rangle\left|\psi_k^{p'}\right\rangle. \tag{4.9}$$

We define $U_k = e^{i\theta H_1^k} e^{i\theta H_0^k}$. Since H_0^k and H_1^k are involutory matrices it follows that $e^{i\theta H_{0,1}} = \cos(\theta)I + i\sin(\theta)H_{0,1}$. Using equations (4.8), (4.9) and the last two we obtain

$$U\left|\psi_k^p\right\rangle = \sum_{p'=0}^{2} \left\langle p'\right|U_k\left|p\right\rangle\left|\psi_k^{p'}\right\rangle. \tag{4.10}$$

Proposition 4.3.3 *Let λ_k^p be the eigenvalues of U_k with eigenvectors $\left|w_k^p\right\rangle$. The eigenvalues of U are λ_k^p with eigenvectors $\left|v_k^p\right\rangle = \sum_{p'=0}^{2} \left\langle p'\right|w_k^p\left\rangle\right|\psi_k^{p'}\left\rangle$.*

Proof

$$U\left|v_k^p\right\rangle = U\sum_{p'=0}^{2} \left\langle p'\right|w_k^p\left\rangle\right|\psi_k^{p'}\left\rangle = \sum_{p'=0}^{2} \left\langle p'\right|w_k^p\left\rangle U\right|\psi_k^{p'}\left\rangle$$

Using equation (4.10) we obtain

$$\begin{aligned} U\left|v_k^p\right\rangle &= \sum_{p'=0}^{2} \left\langle p'\right|w_k^p\left\rangle \sum_{p''=0}^{2} \left\langle p''\right|U_k\left|p'\right\rangle\left|\psi_k^{p''}\right\rangle = \sum_{p''=0}^{2} \left\langle p''\right|U_k \sum_{p'=0}^{2} \left\langle p'\right|w_k^p\left\rangle\right|p'\left\rangle\left|\psi_k^{p''}\right\rangle \\ &= \sum_{p''=0}^{2} \left\langle p''\right|U_k\left|w_k^p\right\rangle\left|\psi_k^{p''}\right\rangle = \lambda_k^p \sum_{p''=0}^{2} \left\langle p''\right|w_k^p\left\rangle\right|\psi_k^{p''}\left\rangle = \lambda_k^p\left|v_k^p\right\rangle \end{aligned}$$

□

In equation (4.10) we make the product on the right by $\left\langle\psi_k^p\right|$. After this we make a summation on p and an integration on k getting

$$U\int_{-\pi}^{\pi} \frac{dk}{2\pi} \sum_{p=0}^{2} \left|\psi_k^p\right\rangle\left\langle\psi_k^p\right| = \int_{-\pi}^{\pi} \frac{dk}{2\pi} \sum_{p=0}^{2}\sum_{p'=0}^{2} \left\langle p'\right|U_k\left|p\right\rangle\left|\psi_k^{p'}\right\rangle\left\langle\psi_k^p\right|.$$

Using the completeness relation we obtain

$$U = \int_{-\pi}^{\pi} \frac{dk}{2\pi} \sum_{p=0}^{2}\sum_{p'=0}^{2} \left\langle p'\right|U_k\left|p\right\rangle\left|\psi_k^{p'}\right\rangle\left\langle\psi_k^p\right|. \tag{4.11}$$

Equation (4.6) tells us that it is important to calculate U^t. We will prove by induction that

$$U^t = \int_{-\pi}^{\pi} \frac{dk}{2\pi} \sum_{p=0}^{2} \sum_{p'=0}^{2} \Big\langle p' \Big| U_k^t \Big| p \Big\rangle \Big| \psi_k^{p'} \Big\rangle \Big\langle \psi_k^{p} \Big|. \tag{4.12}$$

For $t = 1$ we have the equation (4.11). Suppose this is true for $t = n - 1$. Then we have

$$\begin{aligned} U^n = U^{n-1}U &= \int_{-\pi}^{\pi}\int_{-\pi}^{\pi} \frac{dk}{2\pi}\frac{dk'}{2\pi} \sum_{\substack{p,p',\\ p'',p'''}} \Big\langle p' \Big| U_k^{n-1} \Big| p \Big\rangle \Big| \psi_k^{p'} \Big\rangle \Big\langle \psi_k^{p} \Big| \Big\langle p''' \Big| U_{k'} \Big| p'' \Big\rangle \Big| \psi_{k'}^{p'''} \Big\rangle \Big\langle \psi_{k'}^{p''} \Big| \\ &= \int_{-\pi}^{\pi}\int_{-\pi}^{\pi} \frac{dk}{2\pi}\frac{dk'}{2\pi} \sum_{\substack{p,p',\\ p'',p'''}} \Big\langle p' \Big| U_k^{n-1} \Big| p \Big\rangle \Big\langle p''' \Big| U_{k'} \Big| p'' \Big\rangle \Big| \psi_k^{p'} \Big\rangle \Big\langle \psi_k^{p} \Big| \psi_{k'}^{p'''} \Big\rangle \Big\langle \psi_{k'}^{p''} \Big| \end{aligned}$$

Using statement (4.3.1) we obtain

$$\begin{aligned} U^n &= \int_{-\pi}^{\pi}\int_{-\pi}^{\pi} \frac{dk}{2\pi}\frac{dk'}{2\pi} \sum_{\substack{p,p',\\ p'',p'''}} \Big\langle p' \Big| U_k^{n-1} \Big| p \Big\rangle \Big\langle p''' \Big| U_{k'} \Big| p'' \Big\rangle \Big| \psi_k^{p'} \Big\rangle \delta_{pp'''}\delta(k'-k) \Big\langle \psi_{k'}^{p''} \Big| \\ &= \int_{-\pi}^{\pi} \frac{dk}{2\pi} \sum_{\substack{p,p',\\ p''}} \Big\langle p' \Big| U_k^{n-1} \Big| p \Big\rangle \Big\langle p \Big| U_k \Big| p'' \Big\rangle \Big| \psi_k^{p'} \Big\rangle \Big\langle \psi_k^{p''} \Big| \\ &= \int_{-\pi}^{\pi} \frac{dk}{2\pi} \sum_{p',p''} \Big\langle p' \Big| U_k^{n} \Big| p'' \Big\rangle \Big| \psi_k^{p'} \Big\rangle \Big\langle \psi_k^{p''} \Big| \end{aligned}$$

where we used the completeness relation in the last identity.

As we can see in equation (4.7) our goal is to calculate the n-th moment. So we will use the characteristic function $\Big\langle e^{ik_0\hat{D}} \Big\rangle_t = \Big\langle \psi(t) \Big| e^{ik_0\hat{D}} \Big| \psi(t) \Big\rangle$, where $\hat{D}$ is a transformation such that $\hat{D}\Big|x, y\Big\rangle = x\Big|x, y\Big\rangle$, that is, $\hat{D}$ returns the distance of a computational basis vector to the origin. Using equations (4.6) and (4.12) we get that

$$\Big\langle e^{ik_0\hat{D}} \Big\rangle_t = \int_{-\pi}^{\pi}\int_{-\pi}^{\pi} \frac{dk}{2\pi}\frac{dk'}{2\pi} \sum_{\substack{p,p',\\ p'',p'''}} \Big\langle p' \Big| (U_k^t)^\dagger \Big| p''' \Big\rangle \Big\langle p \Big| U_{k'}^t \Big| p'' \Big\rangle \Big\langle \psi(0) \Big| \psi_k^{p'} \Big\rangle \Big\langle \psi_k^{p'''} \Big| e^{ik_0\hat{D}} \Big| \psi_{k'}^{p} \Big\rangle \Big\langle \psi_{k'}^{p''} \Big| \psi(0) \Big\rangle$$

But

$$\begin{aligned} e^{ik_0\hat{D}} \Big| \psi_{k'}^{p} \Big\rangle &= e^{ik_0\hat{D}} \left(\frac{1}{\sqrt{2}}\right)^{1-\delta_{p0}} \sum_{x=-\infty}^{\infty} e^{-ik'(2x+1-\delta_{p0})} \Big(\Big| 2x+1-\delta_{p0}, 0 \Big\rangle + (\delta_{p0}-1)^{p+1} \Big| 2x+1, 1 \Big\rangle \Big) \\ &= \left(\frac{1}{\sqrt{2}}\right)^{1-\delta_{p0}} \sum_{x=-\infty}^{\infty} e^{-i(k'-k_0)(2x+1-\delta_{p0})} \Big(\Big| 2x+1-\delta_{p0}, 0 \Big\rangle + (\delta_{p0}-1)^{p+1} \Big| 2x+1, 1 \Big\rangle \Big) \\ &= \Big| \psi_{k'-k_0}^{p} \Big\rangle \end{aligned}$$

We use the last two equations and proceed analogously to the inductive step of the calculation of U^t, getting

$$\Big\langle e^{ik_0\hat{D}} \Big\rangle_t = \int_{-\pi}^{\pi} \frac{dk}{2\pi} \sum_{p,p'} \Big\langle p \Big| (U_k^t)^\dagger U_{k^*}^t \Big| p' \Big\rangle \Big\langle \psi(0) \Big| \psi_k^{p} \Big\rangle \Big\langle \psi_{k*}^{p'} \Big| \psi(0) \Big\rangle, \tag{4.13}$$

where $k^* = k + k_0$. Since in our case $\left|\psi(0)\right\rangle = \left|0,0\right\rangle$, we have that $\left\langle\psi(0)\middle|\psi_k^p\right\rangle = \delta_{p0}$. Thus equation 4.13 becomes

$$\left\langle e^{ik_0\hat{D}}\right\rangle_t = \int_{-\pi}^{\pi}\frac{dk}{2\pi}\left\langle 0\middle|(U_k^t)^\dagger U_{k^*}^t\middle|0\right\rangle. \tag{4.14}$$

The characteristic function is constructed in such a way that its n-th derivative with respect to k_0 evaluated in $k_0 = 0$ is the n-th moment in time t. Therefore

$$\begin{aligned}\left\langle \hat{D}^n\right\rangle_t &= \left(-i\frac{\delta}{\delta k_0}\right)^n \left\langle e^{ik_0\hat{D}}\right\rangle_t\Bigg|_{k_0=0}\\ &= \int_{-\pi}^{\pi}\frac{dk}{2\pi}\left\langle 0\middle|(U_k^t)^\dagger\left(-i\frac{\delta}{\delta k}\right)^n U_k^t\middle|0\right\rangle\end{aligned} \tag{4.15}$$

We define $\Lambda_k = \left[\left|w_k^p\right\rangle\right]$ as the matrix 3×3 with columns formed by the amplitudes of the eigenvectors of U_k. Let $D[a_j]$ be the diagonal matrix with entries $a_1, ..., a_n$ on the diagonal, so $U_k = \Lambda_k D\left[\lambda_k^p\right]\Lambda_k^\dagger$. Since $\Lambda_k\Lambda_k^\dagger = I$, we get

$$U_k^t = \Lambda_k D\left[(\lambda_k^p)^t\right]\Lambda_k^\dagger.$$

Then we have $\left(-i\frac{\delta}{\delta k}\right)^n U_k^t = \left(-i\frac{\delta}{\delta k}\right)^n\left(\Lambda_k D\left[(\lambda_k^p)^t\right]\Lambda_k^\dagger\right)$ and using the product rule n times we get

$$\left(-i\frac{\delta}{\delta k}\right)^n U_k^t = \Lambda_k D\left[t^n(\lambda_k^p)^t\left(\frac{\delta\ln(\lambda_k^p)}{i\delta k}\right)^n\right]\Lambda_k^\dagger + O(t^{n-1})$$

because $\left(-i\frac{\delta}{\delta k}\right)^n e^{i\alpha k} = \alpha^n e^{i\alpha k}$ and Λ_k and $\Lambda_k^\dagger$ are not t dependent. Using the last equation in (4.15), using again $\Lambda_k\Lambda_k^\dagger = I$ and $D[a_j]D[b_j] = D[a_jb_j]$ we obtain

$$\left\langle \hat{D}^n\right\rangle_t = t^n\int_{-\pi}^{\pi}\frac{dk}{2\pi}\left\langle 0\middle|\Lambda_k D\left[\left(\frac{\delta\ln(\lambda_k^p)}{i\delta k}\right)^n\right]\Lambda_k^\dagger\middle|0\right\rangle + O(t^{n-1}) \tag{4.16}$$

Therefore to calculate the standard deviation we need the eigenvectors and eigenvalues of U_k.

4.3.2 The eigenvectors and eigenvalues

The matrix U_k has a shape that leads us to make use of algebraic computation. We use the programs wxMaxima[2] and Maple. It is very useful to simplify the matrix U_k and calculate its eigenvalues.

$$U_k = \begin{bmatrix} a_k & b_k & 0\\ b_k & \overline{a_k} & 0\\ 0 & 0 & e^{-i2\theta}\end{bmatrix},$$

[2] wxMaxima is a document based interface for the computer algebra system Maxima

where

$$a_k = \frac{1}{9}\left(4 + 5\cos(2\theta) - 3i\sin(2\theta) - 8e^{i2k}\sin^2\theta\right),$$
$$b_k = -\frac{-4\sqrt{2}i\sin\theta}{9}\left(\sin k\sin\theta - 6\cos k\cos\theta\right).$$

The eigenvalues are

$$\begin{aligned}\lambda_k^0 &= e^{i\phi_k},\\ \lambda_k^1 &= e^{-i\phi_k},\\ \lambda_k^2 &= -e^{-i2\theta},\end{aligned} \tag{4.17}$$

where

$$\cos(\phi_k) = 1 - \frac{2(8\cos^2 k + 1)\sin^2\theta}{9}.$$

We are interested in the derivative of $\ln(\lambda_k^p)$ with respect to k. Note that λ_k^2 does not depend on k so the diagonal matrix of equation 4.16 has a 0 entry in the lower right-hand corner. Thus we can reduce our problem for matrices 2×2. The eigenvectors that are important to us are

$$\left|w_0\right\rangle = \frac{1}{\sqrt{c_k^+}}\begin{bmatrix} b_k \\ e^{i\phi_k} - a_k \\ 0 \end{bmatrix} \text{ and } \left|w_1\right\rangle = \frac{1}{\sqrt{c_k^-}}\begin{bmatrix} b_k \\ e^{-i\phi_k} - a_k \\ 0 \end{bmatrix}, \tag{4.18}$$

where $c_k^\pm = 2(1 - \Re(a_k)\cos(\phi_k) \mp \Im(a_k)\sin(\phi_k))$, $\Re(a_k)$ and $\Im(a_k)$ are respectively the real and imaginary parts of a_k.

As we want to compare our results of the simulations with the analytic expression, we have to divide equation (4.7) by time t as we have done in Figure 21. We have that

$$\frac{\sigma(t)}{t} = \sqrt{\frac{\langle\hat{D}^2\rangle}{t^2} - \left(\frac{\langle\hat{D}\rangle}{t}\right)^2}.$$

Using equations (4.16), (4.17) and (4.18) and making the integration on k we obtain

$$\frac{\langle\hat{D}\rangle}{t} = \frac{4}{3} + \frac{2}{3}\cos^2\theta - \frac{2}{3}|\cos\theta|\sqrt{\cos^2\theta + 8},$$
$$\frac{\langle\hat{D}^2\rangle}{t^2} = \frac{8}{3} + \frac{4}{3}\cos^2\theta - \frac{4}{3}|\cos\theta|\sqrt{\cos^2\theta + 8},$$

Thus,

$$\frac{\sigma(t)}{t} = \frac{2}{3}\sqrt{2 - 9\cos^2\theta - 2\cos^4\theta + |\cos\theta|\sqrt{\cos^2\theta + 8}(2\cos^2\theta + 1)}$$

In Figure 22 we plot the graph of the last equation and compare it with the results of the simulations. As expected the numerical data has the same value of the analytical expression. The value θ^* that maximizes the standard deviation is

$$\tan\theta^* = 3\sqrt{3}.$$

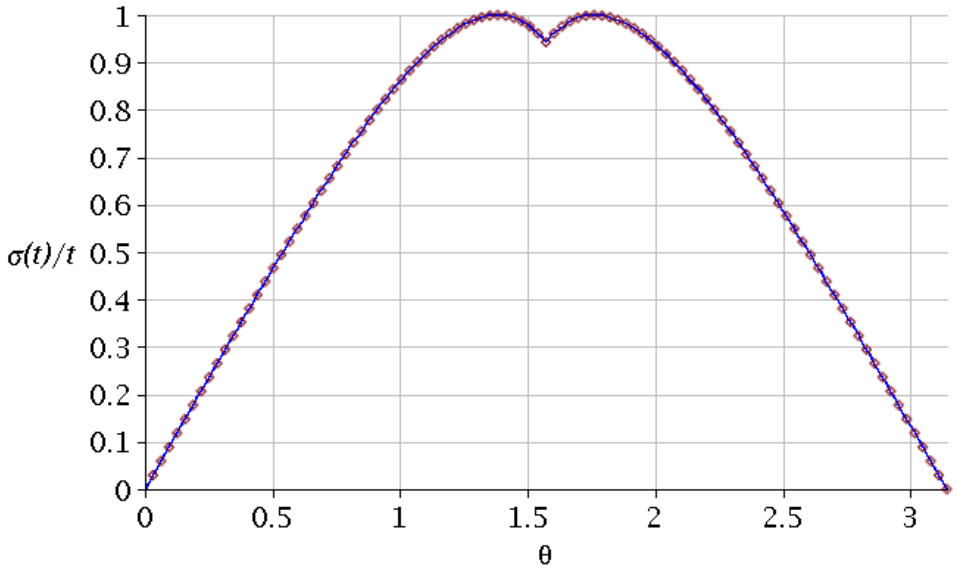

Figure 22 – $\sigma(t)/t$ as a function of θ. The blue curve is obtained from the analytic result and the red diamonds are points observed from the simulations.

5 Conclusion

In this work, we have studied some concepts of graph theory, such as the line graph and the clique graph. These two concepts were very important to prove two theorems. The next concept is the graph tessellation, which is a partition of the vertices of the graph, such that each element of the partition is a clique. If two tessellations cover all edges of a graph G then G is 2-tessellable. Another useful definition is the reduced subgraph, which is a special subgraph of a multigraph. With this, we proved a lemma that was used to show that a graph G is the line graph of a triangle-free (resp. bipartite) multigraph iff $K(G)$ is triangle-free (resp. bipartite). With this we expanded the characterization of the 2-tessellable graphs.

We have also presented coined walks, and described classical and quantum walks on a line and on a general graph. In the classical case the walker tosses a coin, which decides where he goes. So each step is probabilistic. In the quantum case, the walker is in a superposition of positions and after the measurement, the position of the walker is obtained randomly. In all these cases we have a probability distribution. In the line, we have compared the expression of the standard deviation of the classical random walk with the quantum walk. This expression is the same as the expected distance. We showed that in the quantum case the particle walks faster, with a ballistic behavior.

We have also studied another model, the staggered quantum walk. It makes use of the tessellation problem. Each tessellation is associated with a local operator. With this, we define the evolution operator as a unitary operator. We define a tessellation cover of the line of diamonds, which is 2-tessellable because its clique graph is bipartite. Thus we can define the SQW on the line of diamonds. We used the computer program Hiperwalk to simulate the SQW and have obtained the standard deviation for different Hamiltonians. To verify this numerical data we have obtained the analytical expression of the standard deviation. And, with that, we have obtained the best Hamiltonian, that is, $U = e^{i\theta H_1}e^{i\theta H_0}$, where H_0 and H_1 are the local operators and θ satisfies $\tan\theta = 3\sqrt{3}$

For future works, we can obtain the expression of the standard deviation of more general graphs. We can also obtain the expression of the hitting time. Finding the spectral decomposition of 3-tessellable graphs is very helpful to find the standard deviation and the hitting time on such graphs. Another framework is the tessellation problem, where we want to characterize the 3-tessellable graphs.

Bibliography

ABREU, A. et al. The tessellation problem of quantum walks. *CoRR*, abs/1705.09014, p. 124–134, 2017. 13

AHARONOV, Y.; DAVIDOVICH, L.; ZAGURY, N. Quantum random walks. *Proc. R. Soc. Lond. A*, American Physical Society, v. 48, p. 1687–1690, 1993. 13

CHARTRAND, G. *Introductory Graph Theory*. Unabridged. [S.l.]: Dover Publications, 1984. 15

CHILDS, A. M. Universal computation by quantum walk. *Phys. Rev. Lett.*, v. 102, p. 180501, 2009. 13

CHILDS, A. M. et al. Exponential algorithmic speedup by a quantum walk. In: *Proceedings of the Thirty-fifth Annual ACM Symposium on Theory of Computing*. New York, NY, USA: ACM, 2003. (STOC '03), p. 59 – 68. ISBN 1-58113-674-9. 13

DEUTSCH, D. Quantum theory, the church–turing principle and the universal quantum computer. *Proc. R. Soc. Lond. A*, The Royal Society, v. 400, n. 1818, p. 97–117, 1985. 12

FARHI, E.; GUTMANN, S. Quantum computation and decision trees. *Physical Review A*, v. 58, p. 124–134, 06 1997. 13

GROVER, L. K. A fast quantum mechanical algorithm for database search. In: *Proceedings of the Twenty-eighth Annual ACM Symposium on Theory of Computing*. New York, NY, USA: ACM, 1996. (STOC '96), p. 212–219. ISBN 0-89791-785-5. 12

KEMPE, J. Quantum random walks: An introductory overview. *Contemporary Physics*, Taylor & Francis, v. 44, p. 307–327, 2003. 23

PETERSON, D. Gridline graphs: a review in two dimensions and an extension to higher dimensions. *Discrete Applied Mathematics*, v. 126, p. 223 – 239, 2003. 18, 21

PORTUGAL, R. *Quantum walks and search algorithms*. [S.l.]: Springer, 2013. 23

PORTUGAL, R. Staggered quantum walks on graphs. *Phys. Rev. A*, American Physical Society, v. 93, p. 062335, 2016. 17

PORTUGAL, R.; OLIVEIRA, M. C. de; MOQADAM, J. K. Staggered quantum walks with hamiltonians. *Phys. Rev. A*, v. 95, p. 012328, 2017. 13, 35

PORTUGAL, R. et al. "the staggered quantum walk model". *"Quantum Information Processing"*, v. 15, p. 85–101, 2016. 13, 34

SANTOS, R. A.; PORTUGAL, R.; BOETTCHER, S. Moments of coinless quantum walks on lattices. *Quantum Information Processing*, Kluwer Academic Publishers, v. 14, p. 3179–3191, 2015. 39

SHOR, P. W. Algorithms for quantum computation: discrete logarithms and factoring. In: *Proceedings 35th Annual Symposium on Foundations of Computer Science*. [S.l.: s.n.], 1994. p. 124–134. 12

SZEGEDY, M. Quantum speed-up of markov chain based algorithms. In: *45th Annual IEEE Symposium on Foundations of Computer Science*. [S.l.: s.n.], 2004. p. 32–41. 13

VIEIRA, R. *Emaranhamento em Caminhadas Quânticas Desordenadas*. Dissertação (Mestrado) — Universidade do Estado de Santa Catarina, Joinville, SC, 2014. 12